Intersystem Crossing and Nonadiabatic Product Channels in the Photodissociation of N_2O_4 at 193 nm

Julie A. Mueller, Melita L. Morton, Stephen L. Curry, Jonathan P. D. Abbatt,† and Laurie J. Butler*

Department of Chemistry and the James Franck Institute, The University of Chicago, Chicago, Illinois 60637

Received: October 12, 1999; In Final Form: February 9, 2000

This paper presents velocity and angular distribution measurements of the products of N_2O_4 photodissociated at 193 nm. The data show evidence for only N−N bond fission, with no significant branching to N−O bond fission or NO elimination products. The translational energy distribution of the N−N bond fission products is bimodal, indicating that at least two different $NO_2 + NO_2$ product channels contribute significantly to the observed products. Both product channels have an anisotropy parameter of $\beta = 1.7 \pm 0.2$. Using a Franck−Condon-like sudden analysis, we tentatively assign the two fragmentation channels observed as $NO_2(\tilde{X}^2A_1) + NO_2(1^4B_2/1^4A_2)$ and $NO_2(\tilde{X}^2A_1) + NO_2(2^2B_2)$. To further characterize the system we present ab initio calculations (at the level of configuration interaction with single excitations) of the relevant excited states of N_2O_4. The data considered together with the calculations suggest a model for the product branching in which there is spin−orbit coupling in the Franck−Condon region between the excited state, which has mixed singlet $\pi\pi^*$ and $n\sigma^*$ character, and a state with $^3\pi\sigma^*$ character. Branching to the $NO_2(\tilde{X}) + NO_2(1^4B_2/1^4A_2)$ channel occurs upon intersystem crossing to the triplet surface, and formation of the $\pi\pi^*$ diabatic products $NO_2(\tilde{X}) + NO_2(2^2B_2)$ occurs from the singlet $\pi\pi^*$ state nonadiabatic dynamics. Finally, we note that the observed parallel photofragment anisotropy, unexpected for $\pi\pi^*$ electronic excitation of N_2O_4, likely results from vibronic coupling with a $\sigma\sigma^*$ electronic state.

I. Introduction

The photochemistry of the oxides of nitrogen is crucial to the atmosphere, given the role that these species play in the catalytic destruction of O and O_3 in the stratosphere and the production of ozone in the troposphere. Whereas the principal species present in the atmosphere are NO, NO_2, NO_3, and N_2O_5, the photochemistry of related molecules, such as N_2O_4, is of direct interest to the atmospheric chemistry community as well. In particular, N_2O_4 is formed by three-body recombination in any environment where NO_2 is present. In the atmosphere, where NO_2 levels are low, N_2O_4 concentrations are negligible as a result. However, in benchmark laboratory experiments involving nitrogen oxides,[1] where considerably higher reactant concentrations are usually prevalent, N_2O_4 is present at much higher levels. Understanding the photochemical properties of the overall reaction systems requires that the photochemistry of each nitrogen oxide constituent be well studied.

The electronic absorption coefficient of N_2O_4 near 200 nm is over 2 orders of magnitude larger than that of NO_2,[2] allowing us to excite it preferentially in a mixture of the two species. According to the CNDO/S calculations of Mason,[3] excitation of N_2O_4 in the region around 193 nm accesses a potential energy surface of mixed $\pi_{nb,O}\pi_{NO_2}^*/n\sigma_{N-N}^*$ electronic character. The 1^1B_{3u} potential surface to which the planar D_{2h} molecules are excited correlates adiabatically to $NO_2(\tilde{X}^2A_1) + NO_2(1^2B_2)$ products. If we consider a diabatic picture, the electronic configuration with $n\sigma^*$ character correlates to $NO_2(\tilde{X}^2A_1) + NO_2(1^2B_2)$ and the singlet $\pi_{nb,O}\pi_{NO_2}^*$ electronic configuration correlates to $NO_2(\tilde{X}^2A_1) + NO_2(2^2B_2)$. The mixed character of the N_2O_4 excited state arises from the avoided crossing between the $\pi\pi^*$ and $n\sigma^*$ diabatic states in the Franck−Condon region. Molecules such as nitromethane and nitric acid have potential surfaces that are qualitatively similar to those of N_2O_4 along the $R-NO_2$ reaction coordinate.[4,5] However, because the $R-NO_2$ bond is considerably shorter in these molecules than in N_2O_4, the Franck−Condon region is further away from the region of avoided crossing in nitromethane and nitric acid, in which the excited state accessed at 193 nm has almost exclusively $\pi\pi^*$ electronic character. The character of the excited state of N_2O_4 in the Franck−Condon region has been probed in our laboratory[6] by a recent emission spectroscopy study of dissociating N_2O_4 excited near 200 nm. We discuss the results of this work further in section IV.

Studies of the photodissociation of nitromethane and of nitric acid at 193 nm have demonstrated the importance of nonadiabaticity in the $R-NO_2$ bond fission reaction. In nitric acid, the $HO-NO_2$ bond fission products evidence two distinct kinetic energy distributions.[7,8] One was assigned[7] to the adiabatic products, $OH + NO_2(1^2B_2)$, but the other channel forms NO_2 in a higher excited state via an electronically nonadiabatic transition from the $2^1A'$ potential energy surface to another potential surface during the dissociation. Reexamination[7] of earlier results from the nitromethane dissociation[9] revealed a similar pair of H_3C-NO_2 bond fission channels. Since the $R-NO_2$ bonds in nitric acid and nitromethane are quite strong,[7,9] excitation with 193 nm radiation provides insufficient energy to create the $\pi\pi^*$ diabatic products, $R + NO_2(2^2B_2)$. (Although several past studies of the nitromethane dissociation[10,11] state that the $R + NO_2(2^2B_2)$ channel is energetically accessible at

† Department of Geophysical Sciences, University of Chicago, Chicago, IL 60637.

10.1021/jp993651u CCC: $19.00
Published on Web 04/27/2000

193 nm, they used results of theoretical calculations that underestimate the $NO_2(2^2B_2)$ state energy.) In contrast, the weak (12.69 kcal/mol)[12] N−N bond in N_2O_4 means that the $\pi\pi^*$ diabatic products, $NO_2(\tilde{X}^2A_1) + NO_2(2^2B_2)$, are energetically accessible. Thus, this experiment on N_2O_4 provides the opportunity to test whether the $\pi\pi^*$ diabatic products will be found in the photodissociation when that channel is energetically available. It also allows us to assess the importance of spin−orbit coupling in accessing quartet products, as $NO_2(1^4B_2)$ products were considered for the second observed R−NO_2 channel in nitric acid.

Several groups have carried out investigations of the dissociation of N_2O_4 excited at 193 nm. Kawasaki et al.[13] performed photofragment translational spectroscopy experiments and observed emission from the photofragments. They determined that the photofragment recoil kinetic energy distribution at 193 nm is consistent with N−N bond fission forming two electronically excited momentum-matched NO_2 fragments, where the product electronic states could be either 1^2B_2 or 1^2B_1. Although other fragmentation channels (such as $N_2O_4 \rightarrow O + N_2O_3$ and $N_2O_4 \rightarrow NO + NO_3$) are energetically accessible, Kawasaki and co-workers were not able to detect photofragment time-of-flight signal for either NO^+ or O^+, so they could not assess the importance of these other channels. The lack of signal at NO^+ and O^+ is curious, since even the NO_2 product should give daughter ion signal at these masses as a consequence of the electron bombardment used to ionize the photofragments. Geometric constraints preventing quantitative detection of slowly recoiling products also prevented analysis of NO_2 resulting from processes partitioning less than ∼20 kJ/mol of energy into translation.

Sisk and co-workers[14] photodissociated N_2O_4 at 193 nm (as well as at 248 and 351 nm), observing emission from the NO_2 photofragment. They combined their results with the product translational energy distributions determined by Kawasaki et al.[13] and invoked molecular orbital considerations to assign the observed 193 nm dissociation products as $NO_2(1^2B_2) + NO_2(1^2B_2)$.

At this point it is important to note that the calculations of Mason,[3] which were used by both Sisk et al.[14] and Kawasaki et al.[13] to aid in interpretation of their experimental results, were performed with the planar N_2O_4 molecule positioned in the Cartesian coordinate system such that the *x* axis lay along the N−N bond, with the molecule lying in the *xz* plane. The coordinate system used by Sisk et al., Kawasaki et al., and most electronic structure theorists[15−17] also has the molecule in the *xz* plane, but with the *z* axis along the N−N bond. We adopt the latter coordinate system in this work. The difference in axis systems means that vibrational modes, molecular orbitals, and electronic states may have different symmetry labels in the two systems, a fact for which neither Kawasaki et al. nor Sisk et al. accounted. Consequently, many of the arguments they make based on symmetry labels are in error. For example, Sisk and co-workers neglected to transform Mason's label for the state excited at 193 nm; Mason labels the state B_{1u}, which should be transformed to B_{3u} upon changing the coordinate systems. This error means that the argument made by Sisk and co-workers invoking a curve crossing to a state that forms $NO_2(1^2B_2) + NO_2(1^2B_2)$ products is also incorrect.

Similarly, the results of Mason[3] indicate that the transition dipole connecting the N_2O_4 ground state and the 1^1B_{3u} state excited by 193 nm radiation lies along the *z* axis, meaning that the transition dipole moment lies in the plane of the molecule but perpendicular to the N−N bond. However, since the *z* axis lies along the N−N bond in the coordinate system used by Kawasaki and co-workers, that group took the theoretical results to mean that the transition dipole lies parallel to the N−N bond. Consequently, they missed the conflict between Mason's theoretical prediction and their experimental results, which showed the transition dipole moment to be largely parallel to the N−N bond, with an anisotropy parameter, β, of 1.2.

This photofragment translational spectroscopy study of the photodissociation of N_2O_4 at 193 nm addresses the questions raised in the previous studies and attempts to evaluate the importance of electronically nonadiabatic effects in this system as compared to nitric acid and nitromethane. We present product translational energy distributions extracted from the data, as well as the photofragment angular distribution.

II. Experimental Section

These experiments measure the recoil velocity and angular distributions of photofragments from N_2O_4 dissociated at 193 nm. We first collect photofragment spectra using unpolarized light, then polarize the laser beam and take spectra at several polarization angles to measure the angular distribution of the photofragments. The experiments use a crossed laser−molecular beam apparatus with a rotating molecular beam source and universal electron bombardment detector.[18,19]

A 10% mixture of NO_2/N_2O_4 in helium expands into the vacuum chamber through a 127 μm orifice, generating a continuous molecular beam. The pressure of the gas in the stagnation region behind the nozzle is approximately 300 Torr, yielding a mixture in which N_2O_4 comprises 24% of the NO_2/N_2O_4 at 293 K.[2] Proper analysis of the time-of-flight data requires knowledge of the molecular beam velocity and velocity spread, measured by directing the molecular beam straight into the detector and inserting a chopper wheel into its path. This gave an average mean molecular beam velocity of 1110 m/s and a velocity spread ($\Delta v/v$) of 12.7% as given by the full width at half-maximum (fwhm) of the arrival time distribution.

For the first part of the experiment, we focus the unpolarized 193 nm output of a Lumonics PM-848 pulsed excimer laser (set to approximately 3 mJ/pulse) to a 2 mm × 3 mm spot in the interaction region. With each laser pulse, products scatter from the interaction region with laboratory-frame velocities determined by the vector sum of the molecular beam velocity and the recoil velocity imparted during the dissociation. Some of the fragments scatter into the 1.5° acceptance angle of the detector, traveling a total of 44.4 cm to an electron bombardment ionizer that can produce both parent and daughter ions from the neutral photofragments. The electron energy used is 200 eV. The ions are mass-selected by a quadrupole mass filter and then, using a Daly detector in combination with a multichannel scaler, counted as a function of time after the excimer laser pulse.

We collected time-of-flight arrival spectra at several different fragment masses and source-detector angles. For $m/e = 46$ (NO_2^+), we collected 4×10^6 laser shots at a source-detector angle of 10° (at a rate of about 7020 counts of signal per second) and 3×10^6 shots at 15°. We also collected TOF spectra at $m/e = 30$ (NO^+) at an angle of 10° for 2×10^6 shots, and $m/e = 16$ (O^+) at 10° for 7.5×10^6 laser shots at rates of 53000 and 11000 counts/second, respectively. Observation of higher masses could give clues to the relative contribution of $(NO_2)_n$ ($n > 2$) clusters to the total signal. Accordingly, we collected data at a source angle of 0° at $m/e = 92$ ($N_2O_4^+$), $m/e = 76$ ($N_2O_3^+$), $m/e = 62$ (NO_3^+), and $m/e = 60$ ($N_2O_2^+$). No significant signal was apparent; it appears that N_2O_4 and other higher order

clusters are too unstable to withstand the 200 eV electron bombardment and so they all crack to lighter fragments in the ionizer. To assess the contribution from product channels other than $NO_2 + NO_2$, it is useful to compare the NO_2^+, NO^+, and O^+ spectra with those of NO_3^+ and $N_2O_3^+$. Accordingly, we looked for photofragment signal at the masses corresponding to these fragments; nothing was observable at either $m/e = 62$ after one million laser shots or at $m/e = 76$ after two million shots collected at a source-detector angle of 10°.

The second part of the experiment measures the angular distribution of the $m/e = 46$ product. To do this, the unpolarized excimer laser light passes through a single-crystal quartz Pellin−Broca prism that separates it into two linearly polarized components. A half-wave retarder then rotates the horizontally polarized output of the prism to the desired angle. We collected a time-of-flight spectrum with the retarder set to each of six different angles; each spectrum yields one point on the angular distribution plot with a total of 4.5×10^5 laser shots collected at each angle. However, to eliminate the need to normalize for errors due to variation of molecular beam conditions or laser beam intensity, we did not follow a procedure in which all shots were collected for one angle before moving on to the next. Rather, we summed nine sets of TOF spectra in which data were obtained at each angle for 5×10^4 laser shots, varying with each set the order in which the angles were done.

We measure both the molecular beam source and laser polarization angles with respect to the detector axis, but in senses opposite to each other. For example, if a positive angle for the molecular beam source involves a clockwise rotation from the detector axis (clockwise or counterclockwise of course depends on the direction from which the apparatus is viewed), then positive angles of the laser polarization angle involve counterclockwise rotation from the detector axis.

III. Results

Our data show that the only significant primary dissociation process is N−N bond fission, although some of the NO_2 products are formed with enough internal energy to undergo secondary dissociation. The N−N bond fission results in at least two different product channels, which are assigned in section IVA. The upper plot in Figure 1 shows the time-of-flight spectrum obtained for $m/e = 46$ (NO_2^+) at a source-detector angle of 10° with a room temperature molecular beam nozzle. Note that the spectrum is composed of two main peaks, one at relatively short arrival times and the other coming in at longer times. Retaking the spectrum with a nozzle temperature of approximately 35 °C (lower plot in Figure 1), we see that the slow peak arriving near 450 μs decreases significantly in intensity. Although the slightly higher nozzle temperature causes a corresponding increase in molecular beam velocity, the predicted change in the relative heights of the peaks in the TOF spectrum is calculated to be negligible if both peaks result from N_2O_4 photodissociation. However, at the elevated temperature, the slow peak is reduced in intensity by more than 40% relative to the fast one. Therefore, it must result from photolysis of higher-order clusters whose concentration is depleted more than that of N_2O_4 in the expansion at the higher nozzle temperature. Figure 2 shows the $m/e = 46$ (NO_2^+) TOF spectrum collected at 15°. We determined a product translational energy distribution, $P(E_T)$, for the $NO_2 + NO_2$ dissociation channel using a forward convolution fit to the data in Figures 1 and 2 (not fitting the signal shown to result from higher order clusters); the $P(E_T)$ shown in Figure 3 gives the fits shown in Figures 1 and 2. To confirm that the signal results from NO_2 neutral photofragments

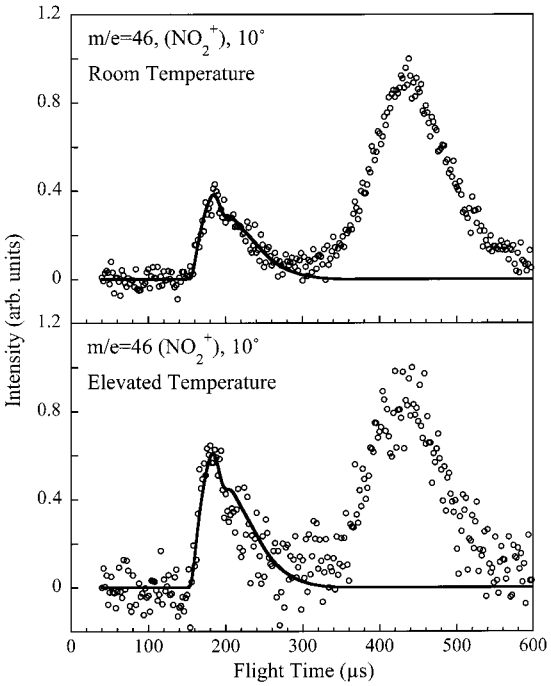

Figure 1. TOF spectra of NO_2^+ collected at a source-detector angle of 10° with the molecular beam nozzle at two different temperatures. The solid lines show forward convolution fits generated using the $P(E_T)$ shown in Figure 3. The difference in the fast:slow peak height ratio indicates that the slow peak results from photodissociation of higher order clusters.

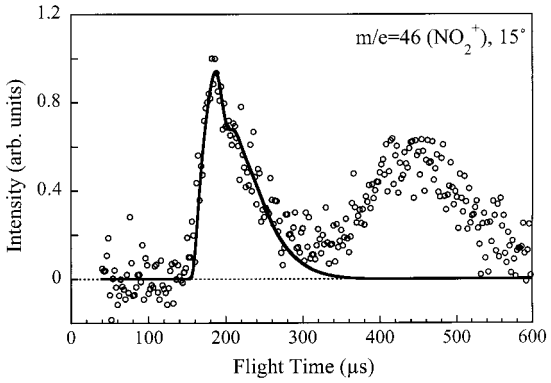

Figure 2. TOF spectrum of NO_2^+ collected at a source-detector angle of 15°. The solid line again is the forward convolution fit generated using the $P(E_T)$ shown in Figure 3.

formed by N−N bond fission, we took spectra for the NO^+ and O^+ daughter ions. There was no significant signal at NO_3^+ and $N_2O_3^+$ (see section II). Figure 4 gives the TOF spectra for $m/e = 16$ (O^+) and $m/e = 30$ (NO^+), with the arrival times corrected for the ion flight time through the quadrupole mass filter. (All the other spectra shown in this paper are raw data; no ion flight times have been subtracted.) Once this correction has been made, a direct comparison can be made of the shapes of the two spectra.

Any peaks appearing in the NO^+ or O^+ spectra that do not appear in the NO_2^+ spectrum would indicate either the existence of another N_2O_4 dissociation channel or contribution to the signal from dissociation of NO_2. However, although NO_2 is favored in the equilibrium between NO_2 and N_2O_4 under the conditions existing in the stagnation region behind our nozzle, the photodissociation of NO_2 clearly does not contribute significantly to our TOF spectra. There are no peaks in the NO^+ and O^+ spectra that do not appear in the NO_2^+ spectrum; the peaks

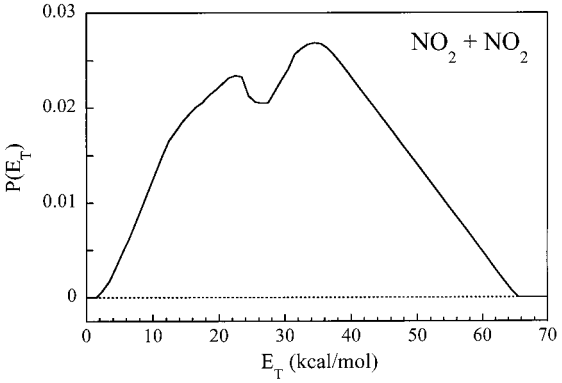

Figure 3. Product translational energy distribution, $P(E_T)$, used to fit the data shown in Figures 1 and 2. The accuracy in determining recoil energies is roughly 2 kcal/mol.

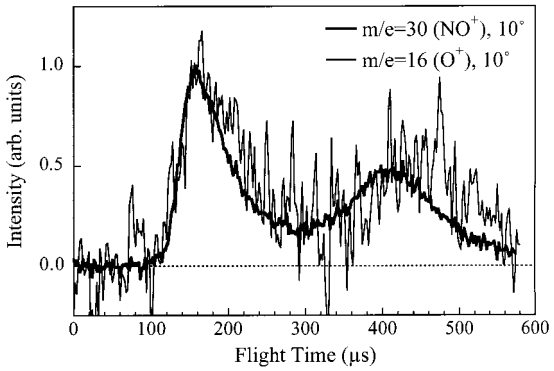

Figure 4. TOF spectra of O^+ (fine line) and NO^+ (heavy line) collected at a source angle of 10°. The spectra have been corrected for the flight times of the ions through the quadrupole mass filter. Note that the fast peak in the O^+ spectrum is slightly wider than the corresponding peak in the NO^+ spectrum, indicating secondary dissociation of some of the NO_2 primary product (see text for details).

in the former spectra are centered at the same arrival time as the corresponding peaks in the latter spectrum, which cannot come from the continuous NO_2/N_2O_4 expansion. The lack of contribution from NO_2 photodissociation is not surprising since the absorption coefficient of N_2O_4 at 193 nm is well over 2 orders of magnitude greater than that of NO_2.[2] The absence of photofragment signal at NO_3^+ and $N_2O_3^+$, combined with the essentially similar appearances of the O^+, NO^+, and NO_2^+ spectra also mean that the only significant primary channel in the dissociation of N_2O_4 excited at 193 nm is $N_2O_4 \rightarrow NO_2 + NO_2$.

Although the signal-to-noise ratio is limited, the spectra in the upper part of Figures 1 and 2 show a fast peak arriving near 200 μs with a shoulder at $\sim$20−40 μs longer arrival times. Thus, the dissociation of $N_2O_4 \rightarrow NO_2 + NO_2$ evidences a bimodal recoil kinetic energy distribution (shown in Figure 3), suggesting that the dissociation proceeds via at least two distinct product channels. The fast peaks in the NO^+ and O^+ spectra at 10° are centered at the same arrival times as the corresponding peak in the NO_2^+ spectrum (after correction for the mass-dependent ion flight time through the quadrupole mass filter), indicating that they result from the same primary photodissociation process. However, closer inspection reveals that the NO^+ and, to a larger extent, the O^+ TOF spectra are broader than the NO_2^+ spectrum in the top part of Figure 1. If the primary NO_2 products were all arriving intact at the ionizer and the lower-mass fragments were simply formed by cracking in the ionizer, the peaks in the measured TOF spectra for all masses should have exactly the same widths and shapes. The fact that

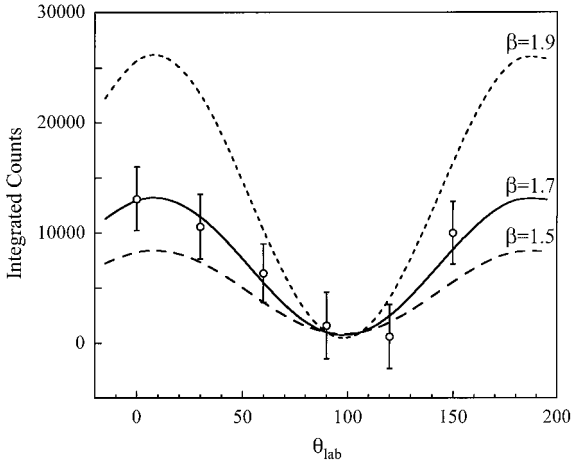

Figure 5. Angular distribution of NO_2 from N_2O_4. Circles show the integrated area of the fast peak of the experimental NO_2^+ TOF spectra collected at each polarization angle. The smooth curves are laboratory-frame distributions simulated using $\beta = 1.5$, 1.7, and 1.9, as indicated. An anisotropy parameter of $\beta = 1.7 \pm 0.2$ gives the best fit to the data.

they do not indicates that some of the NO_2 products underwent secondary unimolecular dissociation, yielding O and NO fragments with a broader range of laboratory velocities than the NO_2 as a result of the additional recoil energy imparted in the secondary dissociation. By conservation of momentum, the O atom will emerge from the NO_2 dissociation with larger velocity than the NO, so comparison of the O^+ and NO^+ TOF spectra in Figure 4 is useful to show the presence of the secondary dissociation. Note that the broadening is very slight, as expected if the secondary dissociation of NO_2 products to NO + O releases little energy to product recoil. Furthermore, the NO^+ spectrum does not show the shoulder that the NO_2^+ spectrum does because the slight recoil of NO from O contributes to the NO^+ spectrum, thus smearing the time-of-arrival distribution.

It is well known that the angular distribution of products from a dissociation can be described in the center-of-mass frame by the classical electric dipole expression

$$I(\theta_{cm}) = 1/(4\pi)[1 + \beta P_2(\cos\theta_{cm})] \quad (1)$$

where θ_{cm} is the angle between the photofragment recoil direction in the center-of-mass reference frame and the electric vector of the linearly polarized light. In the limit of prompt, axial photofragment recoil, the anisotropy parameter, β, is given by

$$\beta = 2P_2(\cos\alpha) \quad (2)$$

where α is the angle between the transition dipole moment for the absorption and the breaking bond. β varies from a value of -1 when the transition dipole moment is perpendicular to the breaking bond (called a "perpendicular" distribution) to 2 when the transition dipole is parallel to the bond (a "parallel" distribution).

Before the expression in Equation 1 can be used to describe the angular distributions obtained in our experiment, it must be converted into the laboratory frame, taking into account the molecular beam velocity distribution, source-detector angle, and the $P(E_T)$ obtained in the experiment performed with unpolarized light. Figure 5 shows the experimentally measured angular distribution of the NO_2 photofragments along with curves simulated using several different values of β in the procedure described above. The individual data points on the plot were

TABLE 1: Experimentally Determined Excitation Energy and Energy Available for Translation for Various Combinations of NO_2 Products

products	T_0 (eV)	$E_{T,max}$ (kcal/mol)	$E_{vertical}$ (eV)	$E_{T,mp}$ (kcal/mol)
$\tilde{X}^2A_1 + 1^2B_2$	1.207[a]	107.4	2.95[e]	67.20
$\tilde{X}^2A_1 + 1^2B_1$	1.83[b]	93.02	2.84[b]	69.73
$\tilde{X}^2A_1 + 1^4B_2/1^4A_2$	unknown		4.49[e]	31.68
$\tilde{X}^2A_1 + 2^2B_2$	4.98[c,d]	20.38	5.22[f]	14.85
$1^2B_2 + 1^2B_2$	2.414	79.55	5.90	insufficient energy

[a] Reference 20. [b] Reference 21. [c] Reference 22. [d] Reference 23. [e] Reference 24. (The data provide a value for vertical excitation to a quartet state. Due to resolution limitations, Rianda and co-workers were unable to distinguish between $^4B_2$ and $^4A_2$, which are predicted to be similar in energy.) [f] Results of reference 23 as interpreted by reference 25.

obtained by finding the area under the fast peak (using limits of 140−250 μs) in the $m/e = 46$ TOF spectra collected with the laser set to the specified polarization angles. By comparing the experimental points with the simulated curves, we see that $\beta = 1.7 \pm 0.2$, which means that the reaction $N_2O_4 \rightarrow NO_2 + NO_2$ gives a largely parallel photofragment angular distribution.

IV. Discussion

A. Assigning $NO_2 + NO_2$* Product Channels. With the measured product translational energy distribution of the $NO_2 + NO_2$ photofragments and the N−N bond dissociation energy, we can use conservation of energy to determine the total amount of energy partitioned into the fragments' internal modes. However, we cannot determine how the energy is distributed among those internal modes. Nevertheless, using known NO_2 excited-state energies along with the O_2N-NO_2 bond dissociation energy ($D_0 = 12.69$ kcal/mol),[12] we can calculate both the maximum energy available for partitioning into translation for each product channel and the most probable translational energy for each channel using a Franck−Condon-like sudden analysis. Calculating the maximum amount of energy available for partitioning into translation simply requires values of T_0, the energy required to excite from the zero-point level of the ground electronic state of NO_2 to the zero-point level of an electronically excited state. T_0 excitation energies for various NO_2 electronic states and the corresponding "maximum available" translational energies ($E_{T,max}$) for those states produced in coincidence with $NO_2(\tilde{X}^2A_1)$ are given in Table 1. It is more instructive, however, to consider not the maximum available energy for product translation but rather the most probable kinetic energy release for each product channel. We assume that the most probable vibrational excitation in the ground or electronically excited product is the one that results when the nascent NO_2 molecule is formed with the geometry it had in ground-state N_2O_4. In other words, the energy of the NO_2 product is determined by vertical excitation to the NO_2 electronic state at the geometry the group had in the intact N_2O_4 molecule. Thus, to arrive at a prediction for the most probable translational energy for each possible product channel, we use literature values of the energies of the various NO_2 electronic states at the geometry of the NO_2 groups in N_2O_4. Since this geometry is almost exactly the same as the equilibrium geometry of $NO_2(\tilde{X}^2A_1)$ ($r_{NO} = 1.195$ Å and ONO angle = 133.7° for NO_2;[26] $r_{NO} = 1.19$ Å and ONO angle = 135.4° for N_2O_4[27]), we can just use the vertical excitation energies of NO_2. These energies are also given in Table 1, and the "most probable" translational energies calculated with them are designated as $E_{T,mp}$. (Reference 24 provides a value for vertical excitation to a quartet state. Due to resolution limitations, Rianda and co-workers were unable to distinguish between $^4B_2$ and $^4A_2$, which are predicted to be similar in energy. Ab initio multireference configuration interaction calculations on the vertical and minimum-to-minimum excitation energies of the doublet and quartet states are presently underway.[28]) This Franck−Condon-like method of course predicts that $NO_2(\tilde{X})$ is formed with no vibrational energy, since the change between the geometry of the NO_2 group in ground-state N_2O_4 and that of free $NO_2(\tilde{X})$ is negligible. However, nascent NO_2 formed in the 1^2B_2 state, for example, is most likely to have vibrational energy considerably in excess of that of the zero-point of the excited electronic state.

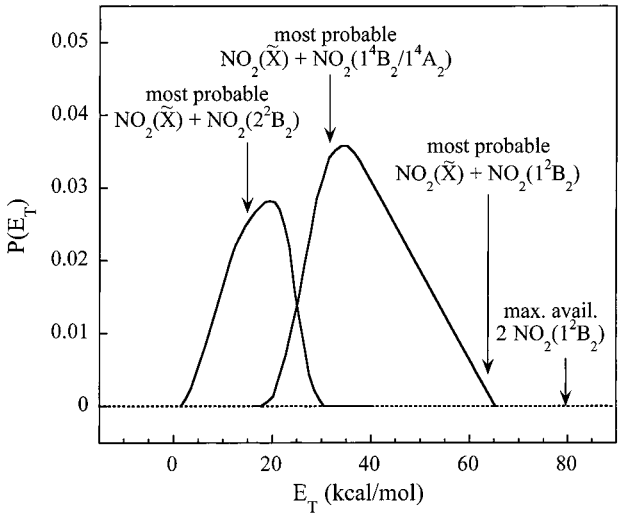

Figure 6. Two distributions extracted schematically from the bimodal $P(E_T)$ shown in Figure 3. The slow and fast distributions peak at 19.50 and 34.62 ± 2 kcal/mol, respectively. When scaled as plotted by the relative probability coefficients for each channel, 34% and 66%, respectively, they give the $P(E_T)$ shown in Figure 3. Arrows indicate maximum available and most probable energies for selected possible combinations of product electronic states, as discussed in the text. Exact values for these energies are given in Table 1.

Figure 6 shows the $P(E_T)$ shown in Figure 3 schematically broken into two separate translational energy distributions. This separation is useful in helping to identify the peaks of the distributions, but the intensities of the individual distributions in the overlap region are not unique. One would expect a calculated $E_{T,max}$ arrow to lie at or beyond the high-energy edge of the translational energy distribution and an $E_{T,mp}$ arrow to lie at the maximum of the distribution if the channel is assigned correctly. As can be seen in Figure 6 and Table 1, the $E_{T,max}$ values are not particularly instructive in this case. The predicted most probable kinetic energy for each possible product channel, the $E_{T,mp}$ values, however, do suggest reasonable assignments for the observed product channels. From their predicted positions, it seems likely that the main products formed in the 193 nm dissociation of N_2O_4 are $NO_2(\tilde{X}^2A_1) + NO_2(1^4B_2/1^4A_2)$ and $NO_2(\tilde{X}^2A_1) + NO_2(2^2B_2)$. The slight broadening of the NO^+ and O^+ spectra indicate that the electronically excited fragments are predissociative, a fact which has been previously reported for the $NO_2(2^2B_2)$ molecule.[22] Previous studies have observed emission from NO_2 in the 1^2B_2 or 1^2B_1 state following N_2O_4 dissociation.[13,14] Although production of NO_2 in these electronic states is not obvious from our work, they could be products with very small quantum yield whose contribution to the translational energy distribution is simply too small to discern. The 1^2B_2 state (which is vibronically very strongly mixed with the high vibrational levels of the 1^2A_1 state) and, to a lesser extent, the 1^2B_1 state emit readily,[20,29] so even small

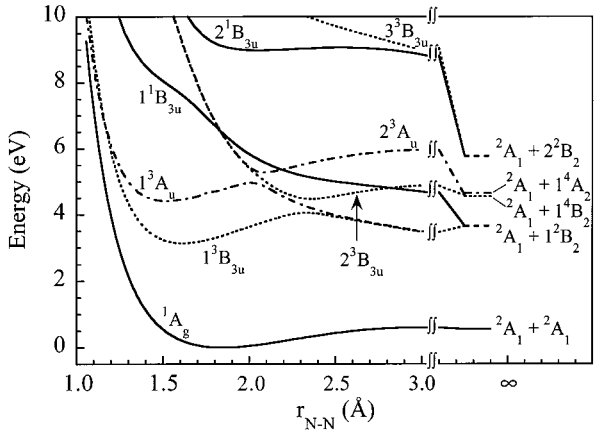

Figure 7. Cuts through N_2O_4 potential surfaces of B_{3u} and A_u symmetry calculated as discussed in the text. Note the crossing between the 1^1B_{3u} and 2^3B_{3u} and 2^3A_u states near $r_{NN} = 1.8$ Å. Also shown (at vertical excitation energies taken from the literature and given in Table 1) are the product electronic states to which the N_2O_4 excited states adiabatically correlate. The apparent energy mismatches between the calculated asymptotic energies and the experimental values result from the relatively low level of theory used in calculating the potential curves.

amounts would be detectable in the previous studies by Sisk et al.[14] and Kawasaki et al.[13] We note that the kinetic energy distribution determined for the $NO_2 + NO_2$ product channel by Kawasaki and co-workers is quite different from ours. Their distribution peaks near 10 kcal/mol and decreases to half of the maximum value at about 35 kcal/mol of total translational energy. It seems likely that the photofragments detected in their TOF spectra included contributions from the dissociation of higher-order clusters in their pulsed-beam expansion.

B. Examining Candidates for an Intersystem Crossing Process Yielding $NO_2(\tilde{X}^2A_1) + NO_2(1^4B_2/1^4A_1)$. Production of $NO_2(\tilde{X}^2A_1) + NO_2(1^4B_2/1^4A_1)$ following excitation of a singlet N_2O_4 state is a spin-forbidden process. Little is known about spin−orbit coupling in N_2O_4. However, if there exists a triplet state of the proper symmetry and with energy similar to that of the initially excited singlet state at the Franck−Condon geometry, the coupling between the two states may be sufficient to cause significant transfer of population from the singlet to the triplet state. Note, however, that the intersystem crossing must happen on a time scale shorter than the rotational period of the molecule at about 50 K, since our measured anisotropy parameter is $\beta = 1.7 \pm 0.2$. Although it is a common assumption that dissociation processes requiring intersystem crossing on a short time scale can be neglected, that assumption cannot hold true in N_2O_4 if we have correctly assigned as $NO_2(\tilde{X}) + NO_2(1^4B_2/1^4A_1)$ the product channel whose kinetic energy release peaks at about 34 kcal/mol. Clearly, we need to reexamine the common assumption that intersystem crossing cannot compete with fast dissociation processes on a singlet state; the case of N_2O_4 is not the first example of this phenomenon.[30,31]

To assess whether there exists a good candidate triplet state for an intersystem crossing product channel, we calculated the triplet excited states of N_2O_4 at the level of configuration interaction with single excitations (CIS) and a 6-311+g(d,p) basis set using *Gaussian 94*.[32] Previous calculations performed in this laboratory for the singlet state used the same basis set and level of theory.[6] Figure 7 shows cuts through both the triplet and the previously published singlet N_2O_4 potential surfaces of B_{3u} symmetry vs the N−N bond length, keeping all other parameters frozen at their N_2O_4 equilibrium positions.[27] For reasons of clarity, we plot only singlet states of B_{3u} symmetry and the two triplet states crossing the 1^1B_{3u} state in the Franck−Condon region, although there are multiple lower and higher lying states of other symmetries. Figure 7 also shows the electronic states of the NO_2 products to which the pictured surfaces correlate adiabatically in D_{2h} geometry (multiple conical intersections change the adiabatic correlations at geometries of lower symmetry). The results of these calculations indicate that the 2^3B_{3u} and 2^3A_u states cross the initially excited 1^1B_{3u} state very close to the Franck−Condon region (gas-phase electron diffraction experiments give values of 1.75−1.782 Å for the N_2O_4 equilibrium bond length[26,27,33]), so one would expect one or the other to play a role in a fast intersystem crossing process. Our preliminary spin−orbit coupling calculations, done with the January 2000 version of GAMESS[34] using single excitations from a CISD ground state wavefunction [6-311g(+)** basis], indicate that the 2^3A_u state has significant coupling (109 cm^{-1}) to the 1^1B_{3u} state in the Franck−Condon region. Significant spin−orbit coupling to the 2^3A_u state, but not the 2^3B_{3u} state, is consistent with the usual expectations outlined by McGlynn.[35] The electronic character of this triplet state (the 2^3A_u) in the crossing region is primarily $\pi\sigma^*$; the 1^1B_{3u} state has just over 50% $n\sigma^*$ character and 40% $\pi\pi^*$ character (combining the contributions of in-phase and out-of-phase configurations) at the crossing point. The 2^3A_u state adiabatically correlates to NO_2 $(\tilde{X}^2A_1) + NO_2$ (1^4A_2) in D_{2h} geometry, since it evolves from $^3\pi\sigma^*$ near the crossing with the singlet state to $^3n\pi^*$ at the product asymptote.

The results thus far suggest a possible mechanism for the branching to the observed product channels. In a diabatic picture, one can view the 1^1B_{3u} state electronic wavefunction at the point of the crossing with the triplet state as a linear combination of the $^1n\sigma^*$ and $^1\pi\pi^*$ diabats (which are coupled by off-diagonal potential coupling). If the $^1n\sigma^*$ and $^3\pi\sigma^*$ diabats are strongly coupled, the portion of the molecular wavefunction with $^1n\sigma^*$ character may preferentially undergo intersystem crossing to the $^3\pi\sigma^*$ diabat and go on to yield the $NO_2(\tilde{X}) + NO_2(1^4A_2)$ products, while the part of the wavefunction with $^1\pi\pi^*$ character results in the $NO_2(\tilde{X}) + NO_2(2^2B_2)$ $\pi\pi^*$ diabatic products observed. This mechanism is purely speculative at this point and requires further investigation. The relative probability weightings required to obtain a good fit to the data using the two $P(E_T)$s shown in Figure 6 are 34% and 66% for the slow and fast distributions, respectively. This result is in general agreement with our model, which predicts 40% and just over 50% for the slow and fast distributions, respectively, if the $n\sigma^*$ configuration contribution to the wave function at the point of crossing results in $NO_2(\tilde{X}) + NO_2(1^4A_2)$ and the $\pi\pi^*$ contribution results in $NO_2(\tilde{X}) + NO_2(2^2B_2)$. More detailed calculations are necessary to assess accurately the importance of spin−orbit coupling in this system and to obtain the necessary input for a full dynamical calculation including spin−orbit coupling to the triplet surfaces.

The mechanism described above for the competition between the $n\sigma^*$ $NO_2(\tilde{X}) + NO_2(1^4A_2)$ channel requiring intersystem crossing and the $NO_2(\tilde{X}) + NO_2(2^2B_2)$ diabatic singlet channel for the $\pi\pi^*$ configuration invites further examination of this group's previous results on nitric acid.[7] Similar to the case of N_2O_4, Myers et al. detected two $HO-NO_2$ bond fission channels. Using the same Franck−Condon-like sudden analysis used here, they assigned the one partitioning larger amounts of energy into translation, and hence less energy into internal modes, to the adiabatic channel analogous to the $NO_2(\tilde{X}) + NO_2(1^2B_2)$ pathway not observed in N_2O_4. In nitric acid, the $2^1A'$ state excited at 193 nm is nearly pure $\pi\pi^*$ in character;

adiabatic traversal of the $\pi\pi^*/n\sigma^*$ avoided crossing near the Franck−Condon region yields adiabatic $OH(\tilde{X}) + NO_2(1^2B_2)$ products. (The second, nonadiabatic $HO-NO_2$ bond fission channel in nitric acid was not definitively assigned. The diabatic $\pi\pi^*$ products, $OH(\tilde{X}) + NO_2(2^2B_2)$, are not energetically accessible upon excitation with 193 nm radiation, so Butler and co-workers[7,30] speculated that this second observed product channel might be $OH(\tilde{X}) + NO_2(1^4B_2)$.) Thus, we were surprised when N_2O_4 dissociation did not result in any singlet-surface adiabatic products, since there is already strong mixing of $\pi\pi^*$ and $n\sigma^*$ character in the Franck−Condon region, making the $NO_2(\tilde{X}) + NO_2(1^2B_2)$ channel more electronically accessible.[36] (Recall that the $n\sigma^*$ state correlates diabatically to $NO_2(\tilde{X}) + NO_2(1^2B_2)$.) The only reasonable explanation for the lack of adiabatic products is that a repulsive triplet state in N_2O_4 lies very near the Franck−Condon region, so in a diabatic picture the flux on the $^1n\sigma^*$ diabat moves via spin−orbit coupling to the triplet state, resulting in $NO_2(\tilde{X}) + NO_2(1^4B_2/1^4A_2)$ products. The remaining flux on the $^1\pi\pi^*$ diabat can evolve to the $NO_2(\tilde{X}) + NO_2(2^2B_2)$ asymptote, the $\pi\pi^*$ diabatic channel that is energetically allowed in N_2O_4 but not in nitric acid.

C. Anomalous Photofragment Angular Distribution. The measured angular distribution of the NO_2 product channel has an anisotropy parameter $\beta = 1.7 \pm 0.2$. This result indicates that the transition dipole for the absorption at 193 nm is nearly parallel to the N−N bond in N_2O_4. Previous work by Kawasaki et al.[13] also reported a parallel anisotropy parameter; their measured value was $\beta = 1.2$, but their data probably included some contribution from higher-order clusters, which would be expected to decrease the anisotropy of the measured distribution. As discussed in the Introduction, the calculations of Mason[3] predict a transition dipole moment lying in the plane of the molecule but perpendicular to the N−N bond. Because of the different coordinate systems used, Kawasaki et al. misinterpreted this result.[13] Consequently, they missed the discrepancy between their results, which showed the angular distribution to be parallel to the N−N bond, and Mason's theoretical results.

Closer examination of the excited electronic configurations of N_2O_4 reveals a possible explanation for the conflicting theoretical and experimental results for the direction of the transition dipole moment. Although the 1^1B_{3u} state is of pure $\pi\pi^*/n\sigma^*$ character in D_{2h} symmetry, at the nonsymmetric geometries occurring as a result of zero-point motion the excited state may include contributions from other electronic configurations with parallel transition moments. In this case, an overall transition moment could result that is intermediate between pure parallel and pure perpendicular. The CIS calculations of singlet excited states previously performed in this laboratory[6] using *Gaussian 94* give a $^1B_{1u}$ state with a vertical excitation energy near 8 eV and a very large oscillator strength, 1.0257. The transition dipole moment connecting this state with the ground electronic state (^1A_g) lies parallel to the N−N bond. The $^1B_{3u}$ state's $\pi\pi^*/n\sigma^*$ electronic configuration can mix with the parallel $\sigma\sigma^*$ configuration ($^1B_{1u}$ in D_{2h} symmetry) at geometries including the zero-point motion of N_2O_4's ν_5 out-of-phase antisymmetric stretch mode,[37] which is of b_{2g} symmetry in our coordinate system. At these geometries, the molecular symmetry is C_{2h}, and the $^1B_{1u}$ and $^1B_{3u}$ states both become ^1B_u. The lower adiabat in this ^1B_u pair retains the primarily $\pi\pi^*/n\sigma^*$ electronic configuration that characterizes the D_{2h} symmetry $^1B_{3u}$ state, but a small amount of $\sigma\sigma^*$ character is mixed in. Although the $\sigma\sigma^*$ contribution to the electronic wavefunction is so small that it is likely unimportant when considering the influence of electronic character on product channels, the oscillator strength associated with the $\sigma\sigma^*$ contribution to the transition moment is very large. As a result, the transition dipole moment rotates to be nearly parallel to the N−N bond, as observed experimentally. Although crude calculations performed using *Gaussian* support it, this explanation awaits confirmation with better electronic structure calculations. CIS calculations such as those performed here can have vertical excitation energies in error by 1 eV or more, so the energies calculated for the $^1B_{3u}$ and $^1B_{1u}$ states are subject to that error. Current emission spectroscopy results,[6] however, also support such a vibronic coupling mechanism, since emission spectra from N_2O_4 excited near 200 nm show progressions in ν_4, the torsional mode, and ν_5, the out-of phase antisymmetric stretch,[37] which result from vibronic coupling of the $^1B_{3u}$ state to a $^1B_{1u}$ state, presumably the same one indicated here.

V. Conclusions

Photofragment translational spectroscopy experiments on the 193 nm photodissociation of N_2O_4 show evidence of two primary N−N bond fission channels, but no significant branching to other bond fission or elimination products. The product translational energy distribution $P(E_T)$ determined from the data for N−N bond fission is bimodal; we tentatively assign the two dominant bond fission channels to $NO_2(\tilde{X}^2A_1) + NO_2(1^4B_2/1^4A_2)$ and $NO_2(\tilde{X}^2A_1) + NO_2(2^2B_2)$. Since the initially excited 1^1B_{3u} state of N_2O_4 correlates adiabatically in D_{2h} symmetry to $NO_2(\tilde{X}^2A_1) + NO_2(1^2B_2)$, branching to both observed product channels requires transitions to other potential surfaces. Formation of $NO_2(\tilde{X}^2A_1) + NO_2(1^4B_2/1^4A_2)$ products requires intersystem crossing, and $NO_2(\tilde{X}^2A_1) + NO_2(2^2B_2)$ are the diabatic products of the $\pi\pi^*$ electronic configuration.

Previous workers[13,14] had detected formation of $NO_2(1^2B_1)$ or $NO_2(1^2B_2)$ by examining emission from the products of the N_2O_4 dissociation. Although this channel is not assigned to either of the dominant product channels in our work, a relatively small fraction of the N_2O_4 molecules could dissociate to give these products. A small contribution may not be discernible as a major peak in our TOF spectra, but because these species fluoresce readily, they would show up clearly in an emission experiment.

Measurement of the angular distribution of the NO_2 products yielded a value for the anisotropy parameter, β, of 1.7 ± 0.2. Calculations by Mason[3] predicted a perpendicular transition dipole leading to the 1^1B_{3u} state believed to be excited upon irradiation by light at 193 nm. The disagreement between theory and experiment can be resolved by recognizing that a state with large oscillator strength and $^1B_{1u}$ symmetry (as labeled for N_2O_4 in D_{2h} symmetry) can mix with the 1^1B_{3u} state upon inclusion of the zero-point motion of the out-of-phase antisymmetric stretch (ν_5). Inclusion of this vibrational motion decreases the symmetry of the N_2O_4 to C_{2h} and allows the two states to couple, giving a transition dipole moment that lies nearly parallel to the N−N bond.

Acknowledgment. This work was supported by the National Science Foundation under grant number CHE-9619376. The authors thank B. F. Parsons for stimulating discussions and help with the ab initio calculations. J.M. gratefully acknowledges support from the Camille and Henry Dreyfus Foundation's Postdoctoral Program in Environmental Chemistry.

References and Notes

(1) See, for example, Schneider, W.; Moortgat, G. K.; Tyndall, G. S.; Burrows, J. P. *J. Photochem. Photobiol. A*, **1987**, *40*, 195.

(2) Bass, A. M.; Ledford, A. E.; Laufer, A. H. *J. Res. Natl. Bur. Stand. (U.S.)*, **1976**, *80A*, 143.
(3) Mason, J. *J. Chem. Soc., Dalton Trans.* **1975**, 19.
(4) Roszak, S.; Kaufman, J. J. *J. Chem. Phys.* **1991**, *94*, 6030.
(5) Harris, L. E. *J. Chem. Phys.* **1973**, *58*, 5615.
(6) Parsons, B. F.; Curry, S. L.; Mueller, J. A.; Ray, P. C.; Butler, L. J. *J. Chem. Phys.* **1999**, *111*, 8486.
(7) Myers, T. L.; Forde, N. R.; Hu, B.; Kitchen, D. C.; Butler, L. J. *J. Chem. Phys.* **1997**, *107*, 5361.
(8) Felder, P.; Yang, X.; Huber, J. R. *Chem. Phys. Lett.* **1993**, *215*, 221.
(9) Butler, L. J.; Krajnovich, D.; Lee, Y. T.; Ondrey, G.; Bersohn, R. *J. Chem. Phys.* **1983**, *79*, 1708.
(10) Moss, D. B.; Trentelman, K. A.; Houston, P. L. *J. Chem. Phys.* **1992**, *96*, 237.
(11) Lao, K. Q.; Jensen, E.; Kash, P. W., Butler, L. J. *J. Chem. Phys.* **1990**, *93*, 3958.
(12) Hisatsune, I. *J. Phys. Chem.* **1961**, *65*, 2249. The value of 13.6 kcal/mol used by some groups as the dissociation energy is ΔH_{298}, generally obtained from Vosper, A. J. *J. Chem. Soc. A.* **1970**, 625, although Hisatsune tabulates a very similar $\Delta H_{298} = 13.64$ kcal/mol. We feel that the comparatively low temperature of our molecular beam warrants use of ΔH_0 rather than ΔH_{298}.
(13) Kawasaki, M.; Kasatani, K.; Sato, H.; Shinohara, H.; Nishi, N. *Chem. Phys.* **1983**, *78*, 65.
(14) Sisk, W. N.; Miller, C. E.; Johnston, H. S. *J. Phys. Chem.* **1993**, *97*, 9916.
(15) von Niessen, W.; Domcke, W.; Cederbaum, L. S.; Schirmer, J. *J. Chem. Soc., Faraday Trans. 2* **1978**, *74*, 1550.
(16) Alrichs, R.; Keil, F. *J. Am. Chem. Soc.* **1974**, *96*, 7615.
(17) Bauschlicher, C. W., Jr.; Komornicki, A.; Roos, B. *J. Am. Chem. Soc.* **1983**, *105*, 745.
(18) Lee, Y. T.; McDonald, J. D.; LeBreton, P. R.; Herschbach, D. R. *Rev. Sci. Instrum.* **1969**, *40*, 1402.
(19) Person, M. D., Ph.D. Thesis, Department of Chemistry, University of Chicago, 1991.
(20) Delon, A.; Jost, R. *J. Chem. Phys.* **1991**, *95*, 5686.
(21) Hardwick, J. L.; Brand, J. C. D. *Chem. Phys. Lett.* **1973**, *21*, 458.
(22) Hallin, K.-E. J.; Merer, A. J. *Can. J. Phys.* **1976**, *54*, 1157.
(23) Coon, J. B.; Cesani, F. A.; Huberman, F. P. *J. Chem. Phys.* **1970**, *52*, 1647.
(24) Rianda, R.; Frueholz, R. P.; Kupperman, A. *J. Chem. Phys.* **1983**, *79*, 5914.
(25) Shih, S.-K.; Peyerimhoff, S. D.; Buenker, R. J. *Chem. Phys. Lett.* **1977**, *46*, 201.
(26) Borisenko, K. B.; Kolonits, M.; Rozsondai, B.; Hargittai, I. *J. Mol. Struct.* **1997**, *413*−*414*, 121.
(27) McClelland, B. W.; Gundersen, G.; Hedberg, K. *J. Chem. Phys.* **1972**, *56*, 4541.
(28) Kedziora, G., private communication of calculations in progress.
(29) Stevens, C. G.; Swagel, M. W.; Wallace, R.; Zare, R. N. *Chem. Phys. Lett.* **1973**, *18*, 465.
(30) See general discussion comment by S. R. Langford and reply by L. J. Butler, *Faraday Discuss.* **1997**, *108*, 327.
(31) See, for example: (a) Reed, C. L.; Kono, M.; Langford, S. R.; Dixon, R. N.; Ashfold, M. N. R. *J. Chem. Soc., Faraday Trans.* **1997**, *93*, 2721. (b) Dixon, R. N.; Hancock, T. W. R. *J. Phys. Chem. A* **1997**, *101*, 7567.
(32) Frisch, M. J.; Trucks, G. W.; Schlegel, H. B.; Gill, P. M. W.; Johnson, B. G.; Robb, M. A.; Cheeseman, J. R.; Keith, T.; Petersson, G. A.; Montgomery, J. A.; Raghavachari, K.; Al-Laham, M. A.; Zakrzewski, V. G.; Ortiz, J. V.; Foresman, J. B.; Cioslowski, J.; Stefanov, B. B.; Nanayakkara, A.; Challacombe, M.; Peng, C. Y.; Ayala, P. Y.; Chen, W.; Wong, M. W.; Andres, J. L.; Replogle, E. S.; Gomperts, R.; Martin, R. L.; Fox, D. J.; Binkley, J. S.; Defrees, D. J.; Baker, J.; Stewart, J. P.; Head-Gordon, M.; Gonzales, C.; Pople, J. A. *Gaussian 94*, Rev. E.2; Gaussian, Inc.: Pittsburgh, PA, 1995.
(33) Smith, D. W.; Hedberg, K. *J. Chem. Phys.* **1956**, *25*, 1282.
(34) Schmidt, M. W.; Baldridge, K. K.; Boatz, J. A.; Elbert, S. T.; Gordon, M. S.; Jensen, J. H.; Koseki, S.; Matsunaga, N.; Nguyen, K. A.; Su, S. J.; Windus, T. L.; Dupuis, M.; Montgomery, J. A. *GAMESS*, January 2000, *J. Comput. Chem.* **1993**, *14*, 1347.
(35) McGlynn, S. P.; Azumi, T.; Kinoshita, M. *Molecular Spectroscopy of the Triplet State*; Prentice-Hall: Englewood Cliffs, NJ, 1969.
(36) Forde, N. R.; Myers, T. L.; Butler, L. J. *Faraday Discuss.* **1997**, *108*, 221.
(37) Bibart, C. H.; Ewing, G. E. *J. Chem. Phys.* **1974**, *61*, 1284.